Scientific Research Publishing

Circuits and Systems, 2026, 17(1), 1-15
https://www.scirp.org/journal/cs
ISSN Online: 2153-1293
ISSN Print: 2153-1285

Realization of Inverse Filters Using IC LT1228 with Grounded Capacitors

Amber Khan[1], Mohd Siddiq Mohsin[1], Mohd Danish Asad[1], Ishanvi Prasad[2], Dinesh Prasad[1*]

[1]Department of Electronics and Communication Engineering, Jamia Millia Islamia, New Delhi, India
[2]Department of Electrical Engineering, Indian Institute of Technology Delhi (IIT), New Delhi, India
Email: *dprasad@jmi.ac.in

How to cite this paper: Khan, A., Mohsin, M.S., Asad, M.D., Prasad, I. and Prasad, D. (2026) Realization of Inverse Filters Using IC LT1228 with Grounded Capacitors. *Circuits and Systems*, **17**, 1-15.
https://doi.org/10.4236/cs.2026.171001

Received: November 15, 2025
Accepted: January 27, 2026
Published: January 30, 2026

Abstract

This paper presents the design and simulation of grounded-capacitor inverse active filters using the LT1228 IC, integrating OTA and CFA for tunable, wideband operation. Inverse filters are characterized by a frequency response that inversely complements that of standard filters. Three filters—Inverse High Pass, Low Pass, and Band Pass—were modeled in Multisim and analyzed in MATLAB. Results confirmed accurate inverse frequency response, ideal for distortion compensation and modern analog signal processing.

Keywords

Inverse Active Filters, LT1228, Operational Transconductance Amplifier (OTA), Current Feedback Amplifier (CFA), Grounded Capacitors, Analog Signal Processing, Electronic Tunability

1. Introduction

Filters are fundamental components in analog signal processing, employed to selectively allow signals of certain frequencies while attenuating others. Traditionally, filters such as low-pass, high-pass, band-pass, and band-stop are utilized for frequency selection and noise suppression in applications ranging from communication systems to biomedical instrumentation. However, in many real-world scenarios, it is not sufficient to simply filter out undesired frequencies; there arises a need to restore or compensate for a distorted signal based on its altered spectral characteristics. In such cases, inverse filters are used to effectively reverse the effects of a system or channel that introduced distortion.

The application of the inverse filter to the output of a given system reconstructs the original input signal (ideally without distortion). Thus, an inverse filter can be defined as a linear filter whose convolution with the original system's impulse re-

sponse yields a delta function:

$$h(t) * h^{-1}(t) = \delta(t)$$

An inverse filter is a main element in many applications, like communications, audio signal processing, instrumentation, etc., where it is used for deconvolution, system identification, and signal restoration. See [1].

An inverse filter is designed to produce a frequency response that is the mathematical inverse of a given standard filter. For example, an inverse low-pass filter attenuates low frequencies while passing high frequencies, in contrast to a conventional low-pass filter. These filters are particularly useful in signal restoration, equalization, and correction tasks, for instance, in communication systems where transmitted signals are distorted by channel characteristics, or in biomedical devices where sensor artifacts need to be removed.

The implementation of inverse filters in analog domain is more challenging compared to digital filters due to component limitations, tuning difficulty, and nonidealities. Active filters offer a solution by using active elements such as operational amplifiers (Op-Amps), operational transconductance amplifiers (OTAs), current feedback amplifiers (CFAs), and other current-mode devices that provide amplification and frequency shaping. Among these, OTA-based and current-mode filters have gained popularity for their advantages in bandwidth, tunability, and compatibility with integrated circuit (IC) design.

Grounded capacitors are a critical choice in modern analog filter design. Compared to floating capacitors, grounded capacitors provide several advantages, such as easier layout, lower parasitic coupling, and better stability. They are more suitable for monolithic implementation, making the filter design more robust and less sensitive to layout-induced interference. Thus, the use of grounded capacitor topologies is highly preferred in IC-level implementations.

The LT1228 is a monolithic analog IC that combines an operational transconductance amplifier (OTA) and a current feedback amplifier (CFA). This hybrid structure enables both voltage-controlled transconductance and high-input impedance voltage buffering within a single chip. The transconductance of the OTA can be adjusted by varying an external bias current (I_{SET}), enabling electronic tunability of filter parameters such as cutoff frequency and quality factor without altering passive components. The CFA stage provides buffering and low output impedance, suitable for cascading stages or driving loads.

The motivation for this project stems from the growing demand for compact, electronically tunable analog filters that can be implemented in integrated form. Inverse filters, while useful, are less commonly studied in practical analog implementations compared to standard filter types. This paper contributes toward filling that gap by proposing grounded-capacitor inverse filters using a widely available analog IC. The findings of this work may have implications in real-time analog signal correction, biomedical filtering, audio equalization, and other adaptive analog systems.

The paper focuses on the design and simulation of inverse active filters using grounded capacitors and the LT1228 IC. Specifically, it aims to realize second-order inverse low-pass (ILPF), inverse high-pass (IHPF), and inverse band-pass filters (IBPF) using minimum components and grounded capacitors only. Each filter topology is designed to exploit the OTA's tunable transconductance for frequency adjustment (where applicable), while maintaining high input impedance and low output impedance via the CFA buffer.

Simulations have been carried out using Multisim for schematic design and circuit behavior, while MATLAB is used to plot and analyze the magnitude versus frequency responses of the filters. This approach allowed verification of theoretical transfer functions and evaluation of frequency tuning capabilities. Component values have been chosen based on design equations to set desired filter characteristics and assess how bias currents affect tunability.

2. Inverse Active Filters (IAFs)

Inverse active filters (IAFs) have gained attention for their ability to compensate signal distortion and perform spectral correction in analog signal processing. Over the years, various active building blocks such as CFOAs, OTAs, and CDBAs have been used to implement these filters, each presenting unique advantages and challenges.

1) CFOA-Based Inverse Filters

Current feedback operational amplifiers (CFOAs) have been extensively utilized in the realization of inverse active filters (IAFs) due to their high slew rate, bandwidth, and simplicity of implementation. Gupta *et al.* [2] proposed four configurations for inverse low-pass (ILP), inverse high-pass (IHP), inverse band-pass (IBP), and inverse band-reject (IBR) filters using AD844 CFOAs, grounded capacitors, and resistors. However, these designs lacked electronic tunability and relied on fixed passive components.

Later, Gupta *et al.* [3] extended this work with more configurations that offered improved impedance characteristics but still used multiple CFOAs. Patil and Sharma [4] proposed two-CFOA topologies to reduce component count, but tunability remained limited. Wang *et al.* [5] introduced a multifunction filter structure capable of realizing several inverse responses through component selection, but only a subset were canonical and practical for integration. Modified CFOA designs like those in [6] aimed to enhance flexibility, but their practical implementation required complex cascading or simulation of non-standard blocks.

2) OTA-Based Inverse Filters

Operational transconductance amplifiers (OTAs) are another common active building block for inverse filter design due to their electronically tunable transconductance (g_m). Tsukutani *et al.* [7] introduced OTA-based ILP, IBP, and IHP filters using grounded capacitors and 5 - 6 OTAs per circuit. These designs offered orthogonal tunability of frequency and quality factor (Q) via bias currents.

More recently, Raj *et al.* [8] proposed five new voltage-mode inverse filter structures using CMOS OTAs and grounded capacitors. These circuits achieved low sensitivity and electronic tunability but required four to five OTA blocks for each configuration, which may pose a challenge for compact integration.

3) CDBA-Based Inverse Filters

Current differencing buffered amplifiers (CDBAs) have also been used to realize inverse filters. Pandey *et al.* [9] proposed a universal configuration using two CDBAs and six admittances to implement all five types of inverse filters. Though functionally rich, this design involved a high number of passive components and floating capacitors.

Nasir and Ahmad [10] suggested a simpler two-CDBA circuit with grounded capacitors but suffered from limited output configurations and unused terminals. Bhagat *et al.* [11] [12] developed multifunctional inverse filter designs that allowed mode selection through switches and provided independent tunability, but their circuits still used multiple CDBAs or CFOA-simulated equivalents, increasing design complexity.

Borah *et al.* [13] presented a sixth-order inverse band-pass filter using CMOS CDBAs. Although highly functional, their design required eight floating capacitors and numerous resistors, making it less suitable for integrated realization.

4) Other Active Elements

Several alternative active elements have been investigated. Herencsar *et al.* [14] employed differential difference current conveyors (DDCCs) to reduce passive component usage. Shah and Malik [15] and Sharma *et al.* [16] used CDTAs to create inverse all-pass and low-pass filters. Kumar *et al.* [17] introduced VDTA-based universal filters that eliminated resistors altogether and used grounded capacitors, enhancing IC compatibility.

While these designs show potential for miniaturization and tunability, they often rely on specialized or complex active elements not readily available in standard IC form.

5) Limitations in Existing Designs

From the above studies, several limitations emerge:

- **Use of floating components**: Many designs (e.g., [9] [12]) use floating capacitors, complicating integration.
- **High active component count**: Designs based on CFOAs or OTAs often require three or more active blocks per filter stage [2] [8].
- **Limited tunability**: CFOA-based circuits lack dynamic tuning capabilities [2]-[4].

6) Present Work with LT1228 IC

The current work overcomes these challenges by using the LT1228 IC, which integrates an OTA and a current feedback amplifier (CFA) in a single package [18]. Its transconductance is electronically tunable via a control current, enabling dynamic adjustment of filter characteristics [19]. The proposed design utilizes only grounded capacitors, making it highly suitable for monolithic implementation. The high input impedance of the CFA section ensures minimal loading, while the OTA allows

frequency tuning by varying the control current.

Unlike previous OTA- or CFOA-based designs, our approach achieves:

- **Reduced component count** using a single active IC per filter.
- **Full electronic tunability** through the control of transconductance for IHPF and IBPF.
- **High integration potential** due to grounded passive elements and simplified topology.

3. Design and Implementation

This section introduces the working principle of the LT1228 integrated circuit (IC) and its application in the implementation of the inverse active filters.

1) Working Principle of LT1228

The LT1228 is a versatile active building block commonly used in analog circuit design due to its combination of an operational transconductance amplifier (OTA) and a current feedback amplifier (CFA) within a single chip. This integration enables both high-performance signal processing and electronic tunability. The OTA's transconductance (g_m) can be precisely controlled by adjusting the external DC bias current (I_B), making the LT1228 ideal for applications requiring dynamic parameter adjustments.

The LT1228 features high input impedance at its voltage input terminals (V^+ and V^-) and low output impedance at the voltage output terminals (x and w), allowing for efficient interfacing with other circuit components. Additionally, the device's current output terminal (y) also exhibits high impedance, facilitating its use in both voltage-mode and current-mode configurations.

The transconductance of the OTA is given by:

$$g_m = \frac{I_B}{3.87V_T} \tag{1}$$

where V_T is the thermal voltage. This tunability can be conveniently managed using a microcontroller or microcomputer, making the LT1228 well-suited for modern, digitally-controlled analog systems.

The LT1228's equivalent circuit and pin diagram, shown in Figure 1 and Figure 2 respectively, highlight its functionality, with an 8-terminal configuration that provides straightforward implementation in analog signal processing tasks.

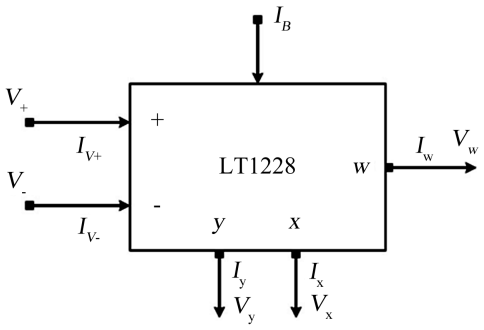

Figure 1. LT1228 symbolic diagram.

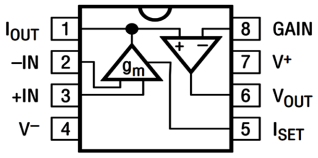

Figure 2. Internal pin diagram of LT1228 (source: datasheet).

The LT1228's electrical behavior can be described using a terminal matrix that relates the input and output currents and voltages. This matrix representation provides insights into how the operational transconductance amplifier (OTA) and current feedback amplifier (CFA) interact within the device.

The usable bias-current range of LT1228 is practically limited to a few hundred μA, beyond which linearity degrades. Bandwidth, though nominally ~100 MHz, is reduced under heavy capacitive loading or high bias. Output stages remain sensitive to resistive/capacitive loads, requiring buffering for stable wide-band operation.

The terminal matrix for LT1228 is given as:

$$\begin{bmatrix} I_{V+} \\ I_{V-} \\ I_y \\ V_x \\ V_w \end{bmatrix} = \begin{bmatrix} 0 & 0 & 0 & 0 & 0 \\ 0 & 0 & 0 & 0 & 0 \\ g_m & -g_m & 0 & 0 & 0 \\ 0 & 0 & 1 & 0 & 0 \\ 0 & 0 & 0 & R_T & 0 \end{bmatrix} \begin{bmatrix} V_+ \\ V_- \\ V_y \\ I_x \\ I_w \end{bmatrix} \tag{2}$$

2) Description of the Filter Circuit

The inverse filters designed in this project use only grounded capacitors and resistors along with LT1228 ICs. This choice ensures ease of integration, low noise susceptibility, and reduced layout complexity. All designs follow a second-order voltage-mode active filter configuration.

a) *Inverse Low-Pass Filter* (*ILPF*): The ILPF attenuates low-frequency components more strongly than high-frequency components, inverting the behavior of a standard low-pass filter. It is implemented as shown in **Figure 3** using two LT1228 ICs, four resistors (R_1 - R_4), and two grounded capacitors (C_1, C_2). The OTA sections of the LT1228 generate currents proportional to the input voltage differences, while the CFA stages buffer these currents into the output node. The high input impedance of the CFA ensures minimal loading on the signal source, and the use of grounded capacitors simplifies PCB layout and improves noise performance. Electronic tunability of the cutoff frequency is achieved by adjusting the bias currents (I_{SET}) of the OTA sections, allowing real-time control without changing passive components.

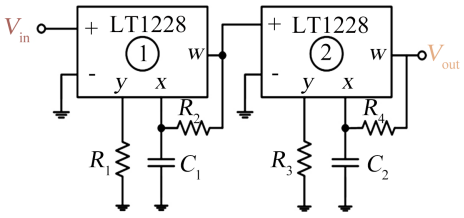

Figure 3. Inverse low-pass filter circuit design.

b) *Inverse High-Pass Filter* (*IHPF*): The IHPF provides attenuation of high-frequency components, passing low frequencies with minimal loss. This inverse of a standard high-pass filter employs two LT1228 ICs, a single resistor, and two grounded capacitors (C_1, C_2) as shown in Figure 4. The OTA stages produce currents that are filtered by the capacitors, and the CFA buffers the resulting signal at the output. The combination of high input impedance and grounded capacitors ensures compatibility with integrated circuits and reduces parasitic effects. As with the ILPF, the cutoff frequency can be tuned electronically via the OTA bias currents, facilitating on-the-fly adjustments.

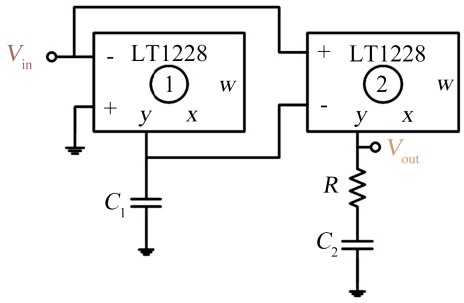

Figure 4. Inverse high-pass filter circuit diagram.

c) *Inverse Band-Pass Filter* (*IBPF*): The IBPF exhibits attenuation around a specified center frequency while passing frequencies outside this band, effectively inverting a conventional band-pass filter response. It uses two LT1228 ICs, four resistors, and two grounded capacitors (C_1, C_2) as shown in Figure 5. The OTA-generated currents flow through the grounded capacitors, shaping the frequency response, and the CFA stages provide buffering with high input impedance. Grounded capacitors minimize layout complexity and parasitic capacitance. Electronic control of the center frequency and bandwidth is achieved by varying the OTA bias currents, offering precise, continuous tuning without altering the passive network.

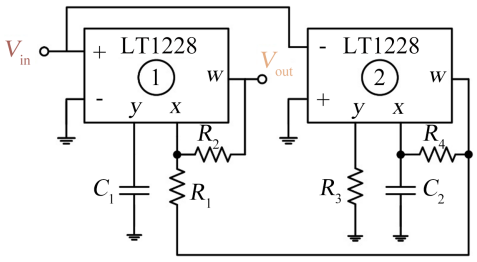

Figure 5. Inverse band-pass filter circuit diagram.

3) Filter Responses

a) *Inverse Low-Pass Filter* (*ILPF*)

Applying the KCL at node *a*, we obtain,

$$I_y = g_{m1} V_{in} = V_a / R_1 ,$$

since $V_y = V_x$,

KCL at *x* of first IC yields

$$V_a\left(sC_1 + 1/R_2\right) = V_w/R_2$$

Applying KCL at node *b*, we get

$$V_w g_{m2} = \frac{V_b}{R_3},$$

KCL at *x* of second IC yields

$$V_b\left(sC_2 + 1/R_3\right) = \frac{V_{out}}{R_4}$$

Upon solving above equations, we get the voltage transfer function of the ILPF as:

$$H_{\text{ILPF}} = \frac{s^2 + s\left(\frac{1}{C_2R_4} + \frac{1}{C_1R_2}\right) + \frac{1}{R_2R_4C_1C_2}}{\frac{1}{g_{m1}g_{m2}R_1R_2R_3R_4C_1C_2}} \tag{3}$$

This form is the reciprocal of a standard second-order low-pass filter. In simulation, the ILPF exhibits deep attenuation at low frequencies, rising toward unity gain in the mid- and high-band as predicted by the numerator and denominator coefficients.

Similarly, the transfer function of IHPF and IBPF can be calculated.

b) *Inverse High-Pass Filter* (*IHPF*): The IHPF transfer function is:

$$H_{\text{IHPF}} = \frac{s^2 + s\left(\frac{g_{m2}}{C_1} + \frac{1}{RC_2}\right) + \frac{g_{m1}}{RC_1C_2}}{s^2\frac{1}{Rg_{m2}}} \tag{4}$$

As the inverse of a high-pass response, this filter shows maximum attenuation at high frequencies with gain increasing toward DC.

c) *Inverse Band-Pass Filter* (*IBPF*): The IBPF is characterized by:

$$H_{\text{IBPF}} = \frac{s^2 + s\frac{1}{R_4C_2} + \frac{g_{m1}\left(R_1 + R_2\right)}{g_{m2}R_2R_3R_4C_1C_2}}{s\frac{R_1}{g_{m2}R_2R_3R_4C_2}} \tag{5}$$

This inverse band-pass response exhibits a notch (deep attenuation) at the design center frequency, with passbands both below and above that notch, exactly opposite to a conventional band-pass filter.

4) Parameter Tunability

A major benefit of the LT1228-based design is that the filter's center or cutoff frequency f_0 can be tuned electronically—by adjusting the OTA bias current I_{SET} without changing any passive components for IHPF and IBPF. However, for ILPF, the frequency is controlled by either R_2 or R_4.

a) *Inverse Low-Pass Filter* (*ILPF*)

$$f_0 = \frac{1}{2\pi}\sqrt{\frac{1}{R_2 R_4 C_1 C_2}} \tag{6}$$

In our ILPF design, the cutoff frequency is set strictly by the resistor–capacitor network (R_2, R_4, C_1, C_2). While the LT1228 OTA still allows electronic adjustment of filter gain, f_0 itself is fixed by the passive values and cannot be shifted via the OTA bias current.

b) *Inverse High-Pass Filter* (*IHPF*)

$$f_0 = \frac{1}{2\pi}\sqrt{\frac{g_{m1}}{RC_1 C_2}} \tag{7}$$

Here, the notch (cutoff) frequency depends on the transconductance (g_{m1}) of the first OTA. Varying I_{SET1} proportionally changes g_{m1}, allowing real-time upward or downward shifts of f_0 without touching any passive parts.

c) *Inverse Band-Pass Filter* (*IBPF*)

$$f_0 = \frac{1}{2\pi}\sqrt{\frac{g_{m1}\left(R_1 + R_2\right)}{g_{m2} R_2 R_3 R_4 C_1 C_2}} \tag{8}$$

In the IBPF, both g_{m1} and g_{m2} control the center frequency, giving two independent knobs (I_{SET1} and I_{SET2}) to adjust f_0.

4. Simulation Results and Conclusions

The proposed inverse active filters—ILPF, IHPF, and IBPF—were simulated using Multisim, and their frequency responses were plotted using MATLAB. Each design was analyzed using practical component values and standard LT1228 bias currents to validate theoretical performance and demonstrate filter behavior.

The component values used for ILPF are:

$R_1 = R_2 = R_3 = R_4 = 1$ kΩ, $C_1 = C_2 = 1$ nF, $I_{SET1} = I_{SET2} = 100$ μA. The Multisim schematic of ILPF is shown in **Figure 6(a)** and the frequency response of the ILPF is shown in **Figure 6(b)**. The response confirms as expected—inverse low-pass behavior. Attenuation is highest at low frequencies, and the gain increases as the frequency rises. Since the ILPF design does not support frequency tuning via bias current, the cutoff frequency remains fixed, matching well with the theoretically calculated value of 159.15 kHz.

The component values used for IHPF are:

$R = 1$ MΩ, $C_1 = C_2 = 100$ pF, $I_{SET1} = I_{SET2} = 100$ μA. The Multisim schematic of IHPF is shown in **Figure 7(a)** and the frequency response of the IHPF is shown in **Figure 7(b)** and it exhibits strong attenuation at high frequencies with gradually increasing gain toward lower frequencies, as expected for an inverse high-pass filter. With the LT1228 OTA's transconductance controlled via bias current, the cutoff frequency can be tuned. At the given bias current, the theoretically calculated value of cutoff frequency is 1.59 MHz.

The component values used for IBPF are:

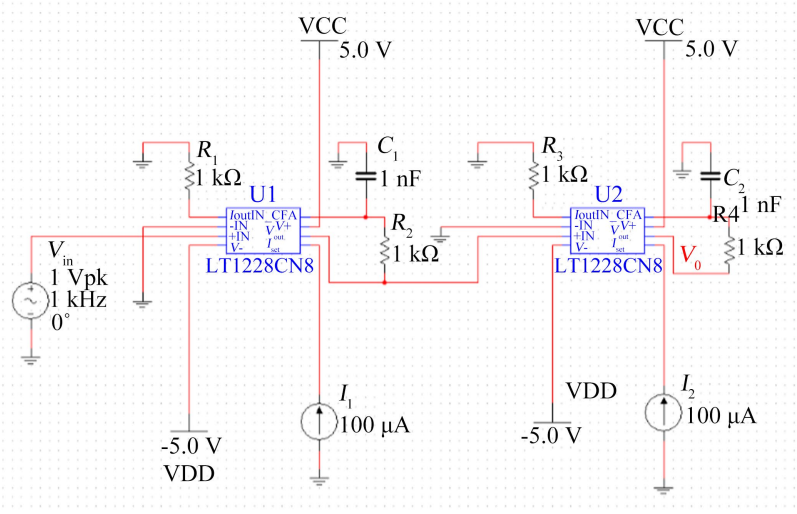

(a)

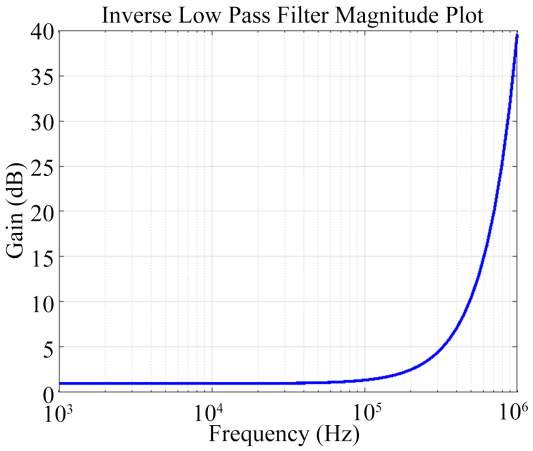

(b)

Figure 6. (a) Multisim schematic of ILPF; (b) Magnitude vs frequency plot for ILPF.

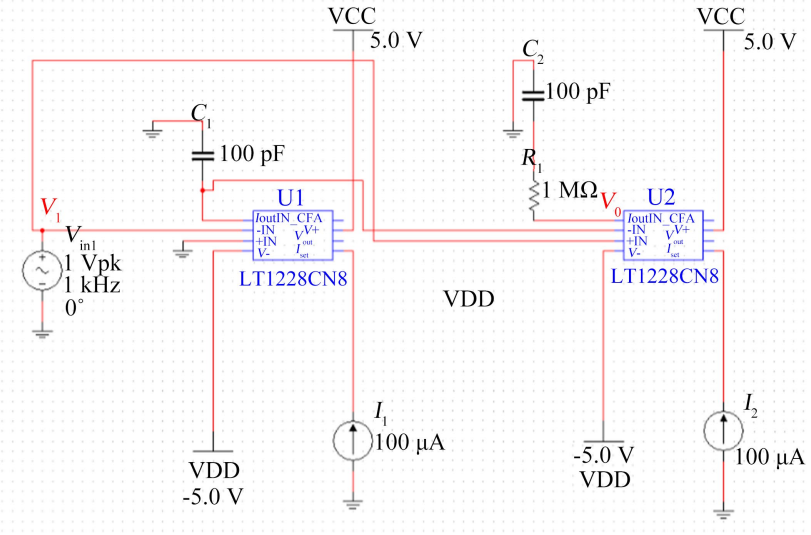

(a)

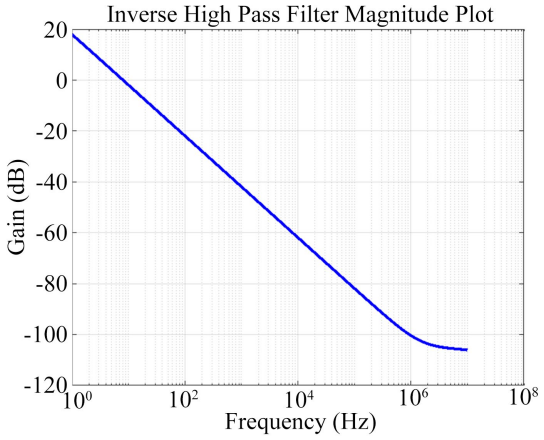

(b)

Figure 7. (a) Multisim schematic of IHPF; (b) Magnitude vs frequency plot for IHPF.

$R_1 = R_2 = R_3 = R_4 = 1$ kΩ, $C_1 = C_2 = 100$ nF, $I_{SET1} = I_{SET2} = 100$ μA. The Multisim schematic of IBPF is shown in **Figure 8(a)** and the IBPF result shown in **Figure 8(b)** demonstrates a clear band-stop (notch) characteristic at a certain mid-frequency. Frequencies outside the notch pass with relatively higher gain. The center frequency, tunable via OTA bias currents, is calculated to be 2.25 kHz.

Each simulation confirms that the filters behave in line with theoretical expectations. The IHPF and IBPF demonstrate clear frequency tunability with respect to bias current settings, whereas the ILPF serves as a fixed-frequency compensating filter. These results validate the design approach and demonstrate the utility of the LT1228 IC in constructing compact, tunable inverse active filters.

To further demonstrate the electronic tunability, the frequency response of the proposed inverse band-pass filter (IBPF) was simulated for three different bias current values of the LT1228 OTA, namely I_{SET1} = 10 μA, 50 μA, and 250 μA. The tunability was analyzed by varying the bias current I_{SET1}, which directly affects the OTA's transconductance and consequently shifts the filter's center frequency.

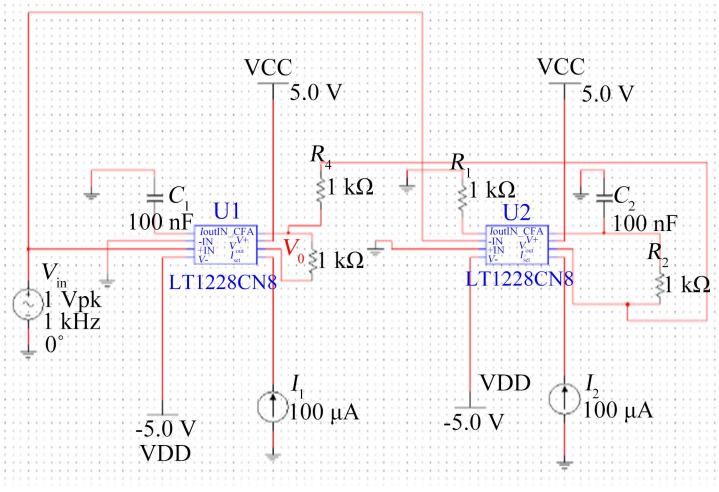

(a)

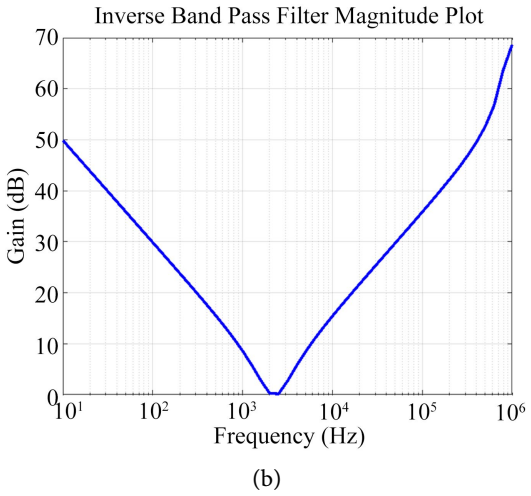

(b)

Figure 8. (a) Multisim schematic of IBPF; (b) Magnitude vs frequency plot for IBPF.

The gain versus frequency plots for the three bias current values were generated in MATLAB using Multisim simulation data, as shown in **Figure 9**. The results clearly illustrate that increasing the bias current increases the transconductance g_{m1}, thereby increasing the filter's center frequency and bandwidth.

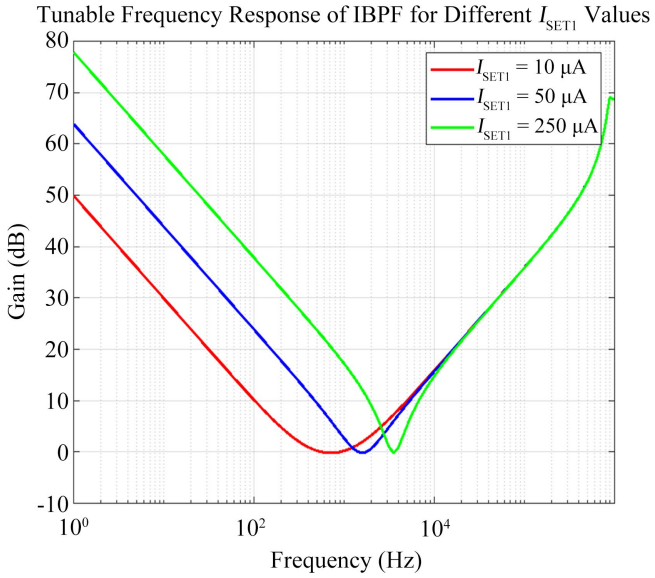

Figure 9. IBPF magnitude vs frequency response for different values of bias currents (ISET1).

Table 1 shows how center frequency shifts with bias current variation and clearly confirms the wide tuning range achievable.

Table 1. Tunability of inverse band-pass filter (IBPF) response.

I_{SET1}	10 µA	50 µA	250 µA
f_0 (kHz)	0.71176	1.591	3.558

Similarly, the response of the inverse high-pass filter (IHPF) can also be electronically tuned by adjusting the LT1228 bias currents I_{SET1} and I_{SET2}, which modulate the OTA transconductance and shift the cutoff frequency accordingly. Both the IBPF and IHPF thus offer dual tunability: their frequency characteristics can be controlled electronically through bias current variation as well as by adjusting passive component values such as resistors and capacitors.

In contrast, the inverse low-pass filter (ILPF) does not support electronic tuning via bias currents and relies solely on passive components for setting its cutoff frequency. This distinction highlights the flexibility and adaptability of the proposed LT1228-based inverse filter designs, enabling dynamic real-time adjustment for IBPF and IHPF while providing a fixed-frequency response with ILPF.

5. Future Work

The present work has successfully demonstrated the design and simulation of second-order grounded-capacitor inverse active filters using the LT1228 IC. However, there remain several opportunities for further development and enhancement of this work.

One immediate direction is the implementation of the filters designed in hardware. While all results in this report are based on simulations in Multisim and MATLAB, building a physical prototype would allow validation of the filters under real-world operating conditions. This would help evaluate the impact of non-idealities such as parasitic capacitance, device mismatch, temperature drift, and noise—factors not fully captured in simulation.

Another important extension involves increasing the order of the filters. The current designs are second-order filters, which are suitable for basic applications. However, more complex signal environments may require higher-order inverse filtering for improved selectivity, sharper roll-off characteristics, and better attenuation. This can be achieved by cascading multiple filter stages or designing active ladder or elliptic structures using LT1228-based cells.

Additionally, while the inverse high-pass and band-pass filters developed here support electronic tunability of the center frequency through OTA bias currents, the inverse low-pass filter (ILPF) lacks this feature in its present form. Future work could focus on modifying the ILPF topology to incorporate tunability without sacrificing its grounded capacitor structure or simplicity.

Exploring these directions would not only validate the robustness of the LT1228-based designs but also expand their applicability in real-time analog signal processing, biomedical instrumentation, and adaptive filtering systems.

Conflicts of Interest

The authors declare no conflicts of interest regarding the publication of this paper.

References

[1] Singh, R. and Prasad, D. (2024) Realization of Filter/Inverse Filter Topologies Using

Single FTFNTA. *Wireless Personal Communications*, **138**, 2469-2488. https://doi.org/10.1007/s11277-024-11610-5

[2] Gupta, S.S., Bhaskar, D.R., Senani, R. and Singh, A.K. (2009) Inverse Active Filters Employing CFOAs. *Electrical Engineering*, **91**, 23-26. https://doi.org/10.1007/s00202-009-0112-3

[3] Gupta, S.S., Bhaskar, D.R. and Senani, R. (2011) New Analogue Inverse Filters Realized with Current Feedback Op-Amps. *International Journal of Electronics*, **98**, 1103-1113. https://doi.org/10.1080/00207217.2010.547812

[4] Patil, V.N. and Sharma, R.K. (2015) Novel Inverse Active Filters Employing CFOAs. *International Journal for Scientific Research & Development*, **3**, 359-360.

[5] Wang, H., Chang, S., Yang, T. and Tsai, P. (2011) A Novel Multifunction CFOA-Based Inverse Filter. *Circuits and Systems*, **2**, 14-17. https://doi.org/10.4236/cs.2011.21003

[6] Garg, K., Bhagat, R. and Jaint, B. (2012) A Novel Multifunction Modified CFOA Based Inverse Filter. 2012 *IEEE 5th India International Conference on Power Electronics* (*IICPE*), Delhi, 6-8 December 2012, 1-5. https://doi.org/10.1109/iicpe.2012.6450471

[7] Tsukutani, T., Sumi, Y. and Yabuki, N. (2014) Electronically Tunable Inverse Active Filters Employing OTAs and Grounded Capacitors. *International Journal of Electronics Letters*, **4**, 166-176. https://doi.org/10.1080/21681724.2014.984636

[8] Raj, A., Bhagat, R., Kumar, P. and Bhaskar, D.R. (2021) Grounded-Capacitor Analog Inverse Active Filters Using CMOS OTAs. 2021 *8th International Conference on Signal Processing and Integrated Networks* (*SPIN*), Noida, 26-27 August 2021, 778-783. https://doi.org/10.1109/spin52536.2021.9566076

[9] Pandey, R., Pandey, N., Negi, T. and Garg, V. (2013) CDBA Based Universal Inverse Filter. *ISRN Electronics*, **2013**, Article ID: 181869.

[10] Nasir, A.R. and Ahmad, S.N. (2013) A New Current-Mode Multifunction Inverse Filter Using CDBAs. *International Journal of Computer Science and Information Security*, **11**, 50-53.

[11] Bhagat, R., Bhaskar, D.R. and Kumar, P. (2019) Inverse Band Reject and All Pass Filter Structure Employing CMOS CDBAs. *International Journal of Engineering Re-search and Technology*, **8**, 39-44.

[12] Bhagat, R., Bhaskar, D.R. and Kumar, P. (2019) Multifunction Filter/Inverse Filter Configuration Employing CMOS CDBAs. *International Journal of Recent Technology and Engineering* (*IJRTE*), **8**, 8844-8853. https://doi.org/10.35940/ijrte.d9476.118419

[13] Borah, S.S., Singh, A. and Ghosh, M. (2020) CMOS CDBA Based 6th Order Inverse Filter Realization for Low-Power Applications. 2020 *IEEE Region* 10 *Conference* (*TENCON*), Osaka, 16-19 November 2020, 11-15. https://doi.org/10.1109/tencon50793.2020.9293817

[14] Herencsar, N., Lahiri, A., Koton, J. and Vrba, K. (2010) Realization of Second-Order Inverse Active Filter Using Minimum Passive Components and DDCC. *Proceedings of 33rd International Conference on Telecommunications and Signal Processing*, Vienna, 17-20 August 2010, 38-41.

[15] Shah, N.A. and Malik, M.A. (2005) FTFN Based Dual Inputs Current-Mode Allpass Inverse Filters. *Indian Journal of Radio & Space Physics*, **34**, 206-209.

[16] Sharma, R., Chaturvedi, A. and Kumar, M. (2015) A Low-Voltage, Low-Power Bulk-Driven Mixer Using 0.18 μm CMOS Technology. 2015 *IEEE UP Section Conference on Electrical Computer and Electronics* (*UPCON*), Allahabad, 4-6 December 2015, 594-601. https://doi.org/10.1109/upcon.2015.7456751

[17] Kumar, P., Pandey, N. and Paul, S.K. (2019) Realization of Resistorless and Electron-

ically Tunable Inverse Filters Using VDTA. *Journal of Circuits, Systems and Computers*, **28**, Article 1950143. https://doi.org/10.1142/s0218126619501433

[18] LT1228: 100 MHz Current Feedback Amplifier with DC Gain Control. Analog Devices. https://www.analog.com/en/products/lt1228.html

[19] Bhaskar, D.R., Raj, A. and Kumar, P. (2019) Mixed-Mode Universal Biquad Filter Using OTAs. *Journal of Circuits, Systems and Computers*, **29**, Article 2050162. https://doi.org/10.1142/s0218126620501625